RSC Advances

ROYAL SOCIETY OF CHEMISTRY

www.rsc.org/advances

Study of a Novel Gel Electrolyte Based on Poly-(methoxy/hexadecyl-poly(ethylene glycol) Methacrylate) Co-polymer Plasticized with 1-butyl-3-methylimidazolium Tetrafluoroborate

Long Wang, Hua-jun Zhu, Wei Zhai, Feng Cai, Xiao-min Liu*
and Hui Yang**

College of Materials Science and Engineering, Nanjing Tech University, 5 Xinmofan Road, Nanjing, Jiangsu, 210009, P. R. China.

Abstract:

Compared with traditional liquid electrolytes, solid polymer electrolytes possess higher reliability and safety but much lower ionic conductivity, which can be improved by incorporating plasticizers to form gel polymer electrolytes (GPEs). However, the commonly employed plasticizers are flammable organic solvents which may cause safety issues. Herein, ionic liquid 1-bultyl-3-methylimidazolium tetrafluoroborate ([Bmim]BF$_4$) is selected as the plasticizer to fabricate inflammable GPE due to its non-volatility and inflammability. The solid matrix is co-polymerized

---

*Corresponding author, Tel/Fax: +86-25-83587762, Email: liuxm@njtech.edu.cn
** Corresponding author, Tel/Fax: +86-25-83587260, Email: yanghui@njtech.edu.cn

from methoxy-poly(ethylene glycol) methacrylate (MPEGM) and hexadecyl-poly(ethylene glycol) methacrylate (HPEGM). The effect of the electrolyte composition on its properties is systematically studied. The synthesized GPEs possess excellent thermal stability and exhibit relatively high ionic conductivity, among which the one named as PMH_{12}-60, composed of 32 wt% MPEGM, 8 wt% HPEGM and 60 wt% $[Bmim]BF_4$, presents an ionic conductivity comparable to liquid electrolytes, up to 1.13×10^{-3} $S\cdot cm^{-1}$ at 30 ℃. In addition, the GPE shows good compatibility with metallic lithium. Furthermore, the coin cell based on PMH_{12}-60, with $LiFePO_4$ cathode and lithium anode shows discharge capacity as high as 145 $mAh\cdot g^{-1}$ and 158 $mAh\cdot g^{-1}$ when cycled at 30 ℃ and 50 ℃, respectively, under the cycling rate of 0.1 C. Moreover, no obvious capacity loss is observed after 30 cycles at both temperatures.

Key words: gel polymer electrolyte; ionic liquid; $[Bmim]BF_4$

Introduction:

Polymer electrolytes in lithium ion batteries have attracted much attention recently due to their fabrication flexibility in shape and size for roll-up displays and wearable electronic devices [1-2], as well as the improvement of reliability and safety compared to the traditional carbonate based liquid electrolytes. The area of solid polymer electrolytes has gone through several developmental stages. The research work was initially carried out on polyethylene oxide (PEO) and/or its derivatives, which can dissolve lithium salts and exhibit high segmental flexibility for ion transport in amorphous phase [3-5]. However, the linear PEO-based solid polymer electrolytes (SPE) present fairly low ionic conductivity (10^{-7}~10^{-8} $S{\cdot}cm^{-1}$) due to their crystallization propensity at temperature below 65 □. Several methods have been proposed to improve the ionic conductivity, including 1) the introduction of polar units [6-10] or non-polar units [11] into the main or side chains to form graft polymer electrolytes (10^{-5} $S{\cdot}cm^{-1}$) and 2) the plasticization of non-aqueous plasticizer into SPE matrix to build gel polymer electrolytes (GPE) with improved ionic conductivity up to 10^{-3} $S{\cdot}cm^{-1}$ [12]. Owing to the high ionic conductivity, organic solvents are widely employed as plasticizers to fabricate GPEs, but their volatility and flammability may cause serious safety issues which might be overcome by introducing non-volatile and nonflammable solvents as plasticizers [13-19]. Recently non-volatile and inflammable room temperature ionic liquids (RTILs) have attracted much attention in electrochemical fields, since many of them exhibit high ionic conductivity and wide electrochemical window [20]. Therefore, RTILs can be considered as novel plasticizers to fabricate GPEs with high safety and superior electrochemical properties. However, Ionic liquids don't behave only as plasticizers. They are able to reduce the polymer host - lithium cation interaction, thus increasing the mobility of the Li^+ ion.

In our previous study [11], a novel polymer matrix named as PMH (Fig. 1) was synthesized by adopting two macro-monomers, methoxyl-poly(ethylene glycol) methacrylate (MPEGM, n=7 or 12) and hexadecal-poly(ethylene glycol) methacrylate (HPEGM, n=7). It has been found that the solid electrolyte copolymerized from 80 wt% MPEGM and 20 wt% HPEGM exhibits relatively high conductivity up to 1.26×10^{-4} $S\cdot cm^{-1}$ at 30 □, indicating that the co-polymer matrix might be a good candidate to fabricate gel polymer electrolytes. The gel polymer electrolyte with non-volatile Tris(methoxypolyethyleneglycol) aluminate ester as plasticizer and PMH as matrix achieves ionic conductivity up to 0.59×10^{-3} $S\cdot cm^{-1}$ at 30 □ [21]. The gel polymer electrolyte prepared with PMH and dual plasticizers (polyethylene glycol dimethyl ether (PEGDME) and polyethylene glycol dilaurate (PEGDL)) exhibits excellent mechanical property and relatively high ionic conductivity up to 0.82×10^{-3} $S\cdot cm^{-1}$ at 30 □[12]. Both studies suggest that PMH can be used to build GPE with high ionic conductivity and superior mechanical property.

In this work, PMH and 1-butyl-3-methylimidazolium tetrafluoroborate ($[Bmim]BF_4$) are used as matrix and plasticizer, respectively, to synthesize novel ionic liquid incorporated gel polymer electrolytes. The effect of the electrolyte composition on its properties, such as thermal stability, glass transition temperature (T_g), and ionic conductivity (σ), is systematically studied. The Li^+ transference number (t_+), lithium/GPE interfacial property and the charge–discharge performance of the built cell based on the synthesized GPE are also measured and discussed in detail. The synthesized GPEs possess excellent thermal stability and exhibit relatively high ionic conductivity, among which the one named as PMH_{12}-60, composed of 32 wt% MPEGM (n = 12), 8 wt% HPEGM and 60 wt% $[Bmim]BF_4$, presents the highest conductivity up to 1.13×10^{-3} S·cm^{-1} at 30 ℃.

Experiment section

1.1 Synthesis of methoxy-poly(ethylene glycol) methacrylate (MPEGM)

Methoxy-poly(ethylene glycol) methacrylate (n=7, 12) were prepared by using methacryloyl chloride to esterify the terminal hydroxyl groups of methoxy poly(ethylene glycol) (MPEG350, 550). The mixture of 0.10 mol MPEG, 0.12 mol TEA and 250 ml dry dichloromethane(DCM) was well stirred at 0 ℃ in an ice-water bath. Methacryloyl chloride (0.12 mol) was added dropwise to the above mixture followed by 12-hour stir. After filtration, vacuum evaporation, and purification through silica gel column with petroleum aether and ethyl acetate at the volume ratio of 5:1 as eluent, a pale yellow product MPEGM was obtained after vacuum desolventizing. The chemical structure of MPEGM is shown in Fig. 1(a) and verified with IR.

1.2 Synthesis of hexadecyl-poly(ethylene glycol) methacrylate (HPEGM)

Hexadecyl-poly(ethylene glycol) methacrylate (n=7) was prepared in a similar method to MPEGM with the following reagents: hexadecyl-poly(ethylene glycol) (HPEG578, 0.1mol), triethylamine (0.12mol), and methacryloyl chloride (0.12 mol). The final product purified through silica gel column is a yellow oily liquid. The chemical structure of HPEGM is shown in Fig. 1(b) and verified with IR.

1.3 Synthesis of ionic liquid [Bmim]BF_4 (IL)

The [Bmim]BF_4 ionic liquid was synthesized by anion exchange in an one-step reaction. The raw chemicals are N-methylimidazolium (99%, Aladdin), 1-bromobutane (≥98%, Aladdin) and sodium fluoroborate (99.99%, Aladdin). The mixture of the above three materials was heated to 80℃ in a stirred three-neck, round-bottom flask under nitrogen for 6 hours till white slurry was obtained. The slurry was kept in vacuum at 100 ℃ for 24 hours before centrifuge several times until the ionic liquid becomes colorless and viscous. The obtained ionic liquid was stored in glove box filled with argon prior to use. The water content in the synthesized IL was measured to be 105ppm by Coulometer (831KF, Netzsch, Germany).

1.4 Preparation of the polymer electrolyte (PMH$_7$, PMH$_{12}$)

The polymer electrolyte PMH$_7$ was prepared in a similar method to PMH$_n$-IL with the following reagents: MPEGM(n=7), HPEGM, azobisisobutyronitrile (AIBN, Aldrich) and LiClO$_4$(99.9%, Aldrich), while the weight ratio of MPEGM(n=7) to HPEGM is 4:1 and the molar ratio of Li to EO is set as 1:20. The polymer electrolyte PMH$_{12}$ was prepared in a similar method to PMH$_n$-IL with the following reagents: MPEGM(n=12), HPEGM, azobisisobutyronitrile (AIBN, Aldrich) and LiClO$_4$(99.9%, Aldrich), while the ratio of MPEGM(n=12) to HPEGM is 4:1 and the molar ratio of Li to EO is set as 1:20.

1.5 Preparation of the polymer electrolyte (PMH$_7$-IL,PMH$_{12}$-IL)

Certain amount of MPEGM(n=7, 12), HPEGM, [Bmim]BF$_4$, azobisisobutyronitrile (AIBN, Aldrich) and LiClO$_4$(99.9%, Aldrich) were dissolved in anhydrous tetrahydrofuran(THF). The mixture of LiClO$_4$ and the PMH$_n$ copolymer at a desired ratio of [Li]:[EO] was stirred for 3 hours in an Ar-filled glove box and then evaporated under reduced pressure for 30 minutes at room temperature to obtain viscous solution. The solution was cast into the Teflon plate and dried at 60 □ under high vacuum for 12 hours to obtain the polymer electrolyte film. This film was cut into disks with 16mm in diameter in an Ar-filled glove box for electrochemical test.

1.6 Physical property (IR, DSC and TGA)

IR spectra were recorded using a TENSOR 27 Fourier transform spectrometer over the range of 4000-400 cm^{-1} at 25 □. ^{1}H NMR spectra of the samples were obtained from a 500 MHz BRUKE NMR spectrometer in chloroform-d. The chemical shifts for ^{1}H-NMR measurements were referred to tetramethylsilane (TMS) as internal standard. ^{13}C NMR spectra were recorded with the same spectrometer in DMSO-d_6.

Thermal analysis was conducted with a DSC200F3(NETZSCH) differential scanning calorimeter over the temperature range from -100 to 100 □ under N_2 atmosphere at the scan rate of 10 □ min^{-1}. The sample, placed in an aluminum container, was first heated to 100 □, then cooled down to -100 □and scanned. Thermogravimetric analysis(TGA) was conducted under nitrogen environment at the heating rate of 10 □ min^{-1} from 25 □ to 500 □ by a TA instrument STA409PC (NETZSCH).

1.7 Electrochemical property

The ionic conductivity of the samples was measured by alternating current(A.C.) impedance spectroscopy using an impedance analyzer (PARSTAT2273) in the frequency range from 0.1 Hz to 10^6 Hz. The polymer electrolyte was sandwiched by two polished stainless steel electrodes, sealed in a testing cell within an Argon-housed dry box. Then the testing cell was measured in the temperature range from 30 ℃to 80℃. The electrical conductivity(σ) can be calculated from the following relation，

$$\sigma = L/R_b \cdot A \qquad (1)$$

where L is the thickness of the sample, A is the cross-sectional area of the sample, and R_b is the bulk resistance obtained from complex impedance plots.

The lithium ion transference number (t_+) of the electrolyte was calculated according to the Evans and Abraham method [22,23] by applying 50mv polarization to the cell, with the following equation,

$$t_+ = \frac{I_s R_{b,s}(\Delta V - I_0 R_{i,0})}{I_0 R_{b,0}(\Delta V - I_s R_{i,s})} \qquad (2)$$

where ΔV is the potential applied across the cell, I_0 and I_s are the initial and steady-state dc current, $R_{b,0}$ and $R_{b,s}$ are the initial and final resistance of the electrolyte, and $R_{i,0}$ and $R_{i,s}$ are the initial and steady-state resistance of the passivating layer.

The electrochemical stability of the electrolyte was determined by Linear sweep voltammetry(LSV) scan using Pt metal as the working electrode and lithium as the counter and reference electrode. The LSV scans were performed at the scan rate of 1 mV·s^{-1} from 2.6 V to 5.4 V vs. Li^{+}/Li at 30 ℃. The interfacial resistance between electrolyte and lithium electrode was analyzed by A.C. Impedance spectroscopy using PARSTAT 2273 impedance analyzer for the Li/GPE/Li cell.

The coin-type(CR2032) lithium polymer cell was prepared using the GPE film, $LiFePO_4$ and metallic lithium(Tianjing Zhongli, China) as electrolyte, cathode and anode, respectively. The cathode ($LiFePO_4$, 99%) was purchased from Changsha Yunchou Power Technology, China (with d_{50} of 4 micron). The content of $LiFePO_4$, conductive acetylene carbon black and PVDF of the fabricated electrode is 91%, 5% and 4%, respectively. In addition, the thickness and diameter of the electrode is 50 micron and 1.3 cm^2, respectively. Furthermore, the active mass loading is measured as about 5 mg.cm^{-2}. The charge-discharge test of assembled cells was carried out using a BT-2000 battery testing system(Arbin, USA) in the voltage range of 2.5-4.0 V versus Li^{+}/Li under 0.1C (0.085 mA.cm^{-2}) rate at both 30 ℃and 50 ℃.

Results and Discussion

1. IR spectra of $[Bmim]BF_4$

Fig. 2 presents the IR spectra of the synthesized $[Bmim]BF_4$. The structural formula of $[Bmim]BF_4$ is shown in Fig. 3. The characteristic bands at 3161.4cm^{-1} and 3121cm^{-1} represent in-phase stretching vibration of C-H (C4, C5) and stretching vibration of C-H (C2), respectively. The characteristic bands at 2938.5 cm^{-1} and 2876.9cm^{-1} correspond to antisymmetrical stretching vibration of $-CH_3$, $-CH_2$ and symmetrical stretching vibration of $-CH_2$, respectively. The peak at 1574.1cm^{-1} is the infrared absorption of the frame vibration of imidazole ring and stretching vibration of C=C. The strong and broad peaks at 1058.0cm^{-1} are due to the frame vibration of C-N and stretching vibration of B-F. The peak at 1171.4 cm^{-1} is attributed to the stretching vibration of N-Bu, N-Me in imidazole ring [24].

2. The glass transition temperature

Fig. 4(a) plots the differential scanning calorimetry curves of various polymer electrolytes and the corresponding polymer matrix PMH_n (n=7, 12). The symbol PMH_n-x represents the gel polymer electrolyte composed of PMH_n (n=7, 12) and the ionic liquid, whileas x stands for the content of the ionic liquid. For example, the sample marked as PMH_{12}-60 contains 60 wt% ionic liquid and PMH_{12} is the polymer matrix.

It is well known that the low glass transition temperature (T_g) is coupled with the high mobility of the EO chains [25]. The T_g of PMH_{12} (-49.2 ℃) is lower than that of PMH_7 (-45.3 ℃), since PMH_{12} with longer EO chains facilitating swing, is of better EO mobility than PMH_7. The T_g of $[Bmim]BF_4$ was reported as -85 ℃ [26]. After $[Bmim]BF_4$ is added as plasticizer, the resulting gel polymer electrolyte presents low T_g compared to the corresponding polymer itself. The addition of ionic liquid lowers crystallization tendency of the polymer and improves the mobility of the EO chains by expanding free volume of the EO chains. In addition, DSC in our measurement of gel polymer electrolyte doesn't exhibit any melting point of the neat IL, agreeing well with what reported in the literature [27]. No crystallization of $BMIMBF_4$ is observed in the DSC scan which might be explained by the difficulties of BMIM cations and BF_4 anions to crystallize due to steric problem arising from the length of alkyl chain [27].

The lithium salt concentration may also have impact on the physical properties of the polymer electrolyte. The PMH_{12}-60 based GPEs containing different amount of lithium salt ([Li]:[EO]=1:12, 1:16, 1:20, 1:24) are compared. The results are plotted in Fig. 4(b). It can be observed that with the increase of the lithium salt concentration, the T_g of the GPE declines first, then goes up after [Li]:[EO] is above 1/20. Initially the presence of small amount lithium salt disrupts the crystallization of EO chains, lowering the glass transition temperature. After [Li]:[EO] is higher than 1/20, the enhanced inter- and intra-molecular coordination between Li^+ and EO units limits the motion of EO chains, resulting in the rise of the glass transition temperature.

3. Thermal properties

The thermal stability of the ionic liquid, solid matrix PMH_n (n=7, 12) and the gel polymer electrolyte PMH_n-x (n=7, 12; x=70, 60, 30) is analyzed by thermogravimetry under N_2 atmosphere and the results are shown in Fig. 5(a) and Fig. 5(b). In the temperature range from 80 □ to 250 □, no mass loss is observed for [Bmim]BF_4, while small amount of weight loss is detected for PMH_n and PMH_n-ILs, presumably caused by the evaporation of low molecular weight components. In the temperature range from 250 □ to 500 □, mass loss of 83 wt% is observed for pure IL corresponding to the decomposition of the IL. In the temperature above 250 □, both the IL and PMH_n decompose in one stage. In contrast, the PMH_n-IL gel polymer electrolytes exhibit two-stage decomposition mechanism. Upon heated up, PMH_n-IL experiences the decomplexation of PMH_n-IL, degradation of PMH, followed by decomposition of the ionic liquid [28]. It can be found that PMH_7-IL decomposes at higher temperature than PMH_{12}-IL, the reason could be that more EO chain presence in PMH_{12}-IL reduces the crystallization propensity and makes it less stable. PMH_n-IL starts to decompose at lower temperature than PMH_n itself. The decomposition temperature of PMH_n-IL decreases with the increase of the ionic liquid at low content, then goes up as shown in both Fig. 5(a) and 5(b). The small amount addition of the ionic liquid disrupts the crystallization in the polymer, and makes the PMH_n-IL less stable and decomposes at lower temperature. When the content of the ionic liquid reaches certain level, the ionic liquid exists in PMH_n-IL in the complex form and also in the free form but enclosed in PMH_n [28]. The existence of the ionic liquid in large quantity stabilizes the PMH_n-IL electrolyte.

4. Ionic conduction

Fig. 6(a) and Fig. 6(b) present the dependence of the conductivity (σ) on 1/T for the PMH_7/PMH_{12} based polymer electrolytes containing plasticizer in the temperature range from 30 ℃ to 80 ℃. The sample cell is equilibrated at the testing temperature for 60 min before-measurement. It can be seen clearly that at higher temperature, all electrolytes present higher conductivity because high temperature promotes the mobility of both EO chains and Li^+ in the IL. The conductivity of PMH_{12} is higher than that of PMH_7 at the same temperature. PMH_{12} shows low T_g and high chain mobility compared to PMH_7. The conductivity is greatly enhanced after IL being plasticized into the PMH_7/PMH_{12} matrix, since the introduction of plasticizer in polymer matrix suppresses the degree of crystallinity [28], encourages the motion of EO chains, lowers the required activation energy, decreases the glass transition temperature and improves the Li^+ conductivity in the polymer electrolytes [12]. More importantly, IL itself presents several orders higher conductivity than both polymer matrices. This is also the main reason that at the same temperature and based on the same matrix, the electrolyte with more IL exhibits higher conductivity. The second reason lies in the reality that the introduction of plasticizer enhances free volume expansion of the EO chains. With the same amount of IL plasticized, the PMH_{12} based electrolyte presents higher σ than the PMH_7 based electrolyte. The gel polymer electrolyte containing more IL possesses better ionic conductivity, but may exhibit poor mechanical stability. Considering the mechanical strength and conductivity (1.13×10^{-3} $S\cdot cm^{-1}$), PMH_{12}-60 is selected for electrochemical performance evaluation.

5. Transference number measurement

The bulk and interfacial resistance of the Li/PMH_{12}-60/Li cell before and after polarization is measured by A. C. impedance. The results are plotted in Fig. 7. The inserted figure is the depolarization curve of the cell subjected to small DC polarization potential (50 mV) for sufficient time to reach steady-state. The data related to the t_+ calculation is summarized in Table 1. Generally speaking, comparing two similar systems at the same temperature, the one with high resistance exhibits large transference number [29]. The measured t_+ values of these polymer electrolytes are between 0.26 and 0.35 (less than 0.5), suggesting that the contribution of Li^+ to the total ionic conductivity is much less than the other ions, which is in good agreement with what reported in many gel polymer electrolyte studies [12,30]. The gel electrolyte plasticized with IL exhibits a sightly higher t_+ value than the corresponding solid polymer electrolyte. Moreover, the electrolyte plasticized with more IL is of higher t_+ value.

6. Interface stability resistance between lithium electrode and polymer electrolyte

The interfacial compatibility of the gel electrolyte with metallic lithium is a key factor since uncontrollable passivation on the lithium electrode may cause serious safety issues. The prepared ionic liquid and PMH matrix may contain trace amount of residual impurities and/or moisture which may increase the interfacial resistance between lithium electrode and electrolyte. In this study, the interfacial stability is analyzed by measuring the A. C. impedance of a Li/PMH_{12}-60/Li coin-typed cell stored at room temperature under open circuit potential condition. Fig. 8(a) presents the Nyquist spectra and Fig. 8(b) shows the change in the area specific bulk (R_{bulk})

and interface resistances (R_{intf}) as a function of storage time. Generally, the interface between the polymer electrolyte and the Li electrode may exhibit high resistance up to the order of 10^3 Ω [19,31], due to imperfect contact and the formation of a passivation layer on the lithium electrode. In this study, R_{bulk} and R_{intf} in the fresh cell are 180 $\Omega\cdot cm^2$ and 556 $\Omega\cdot cm^2$, respectively. R_{bulk} increases slightly and stabilizes at 400 $\Omega\cdot cm^2$ after 12 days storage. This increase can be ascribed to the formation and growth of the passivation layer which affects the nature of the polymer electrolyte [32]. In contrast, R_{intf} jumps in the first 72 hours, then decreases slightly along the time before 96 hours, afterwards it levels up to 1600 $\Omega\cdot cm^2$ in the next 72 hours before stabilizing. The initial sharp increase of the R_{intf} can be mainly attributed to the formation and growth of the passivation layer. Moreover, the trace amount of residual moisture and/or impurities (such as ethylene glycol) might react with Li to produce LiOH, Li_2O and other Li organic compounds to increase the interfacial resistance [33]. The decrease of the interfacial resistance during 72-96 hours might be claimed to the formation of an ion-conducting polymer layer produced by the reaction between Li and ester groups of PMH. This polymeric layer may prevent the corrosion of lithium electrode from the impurities. After 288 hours, R_{intf} reaches the steady value of 1680 $\Omega\cdot cm^2$, indicating that the PMH_{12}-60 electrolyte is compatible with the lithium electrode well. The change of R_{intf} and R_{bulk} along the storage time suggests that the composition of the gel polymer electrolyte may be altered by the possible reactions between GPE/impurities and lithium electrode.

7. Electrochemical stability of the polymer electrolytes

The electrochemical stability of the electrolytes (PMH_{12}-60), is studied by cyclic voltammogram scans with Pt as the working electrode and Li as the reference/counter electrodes (Fig. 9). With the extremely slow scan rate in this study (0.2 $mV.s^{-1}$), very small distance between the working and counter/reference electrode (50 µm), and a thick piece of metallic lithium as reference/counter electrode (which can keep the voltage of counter/reference side constant), it can be concluded that the IR drop in this experiment can be neglected. The obtained polymer electrolyte has a stable electrochemical window more than 4.5 V, suggesting that it can be applied to the practical lithium polymer battery [34]. Nishida et al. also pointed out that 1-alkyl-3-methylimidazolium tetrafluoroborate has an electrochemical window of about 4 V measured via a three electrode cell. [27] Even though the reduction of most dialkylimidatizoliums generally takes place at around 0.6 V to 1 V vs. Li^+/Li [27, 35], they can find application in the $Li_4Ti_5O_{12}$ or lithium alloys based Li-ion cells.

8. Cell testing

A Li/PMH$_{12}$-60/LiFePO$_4$ based 2032 coin cell is cycled at 0.1C (1C = 170 mA·g^{-1}) for 30 cycles at both 30 □ and 50 □. The discharge capacity versus cycle number at different temperature is presented in Fig. 10(a) and Fig. 10(b), respectively. The charge-discharge curves of the 1st, 15th and 30th cycle are exhibited in the inseted figures. As shown in Fig. 9(a), the discharge capacity is 125 mAh·g^{-1} in the first cycle, gradually increases to 145 mAh·g^{-1} during the initial 10 cycles, which can be explained as that the penetration of the ionic liquid from membrane to the porous electrode makes full utilization of the active materials [36]. The coulombic efficiency is 95.2% in the 1st cycle and 98% in the following cycles. The irreversible capacity observed during these cycles is consumed in passivating the surface of the metallic Lithium [37]. As we discussed in the previous part, it takes some time to form a stable passivate film in the electrode/electrolyte interface. However, when the cell is cycled at 50 □, the discharge capacity is 158 mAh·g^{-1} (close to the theoretical value) in the first cycle, remains stable and presents no capacity fade after 30 cycles. The coulombic efficiency maintains at 92.3 % in all 30 cycles. At elevated temperature, both transport and reaction kinetics are promoted, resulting in the improvement of discharge capacity. Moreover, side reactions from the residue impurities and lithium are also enhanced, which reduces coulombic efficiency. At both temperatures, slightly oblique curves are observed for all presented charge/discharge curves, which is different from the normal charge/discharge curves for $LiFePO_4$. The possible reason is explained as follows. The transport of all ions in electrolyte contributes to the ionic conductivity, but only the transport of Li^+ is relevant to the charge/discharge processes within a Li-ion cell. In polymer electrolyte plasticized with $[Emim]BF_4$, it was reported that $Emim^+$ has higher self-diffusion rate than Li^+ [38], which means that Li^+ diffuses slower than $Emim^+$. Hayamizu et al. proposed that the Li^+ and anion form ion complexes and diffuse together while $Emim^+$ becomes relatively free to move. But the transport of other ions may lead to cell polarization, which might cause the charge/discharge curves deviate from plateau [39]. The excellent cycling performance at low current at both temperatures can be ascribed to the relatively high conductivity of the PMH_{12}-60 gel electrolyte [40], as well as the good compatibility between PMH_{12}-60 and metallic Lithium [41].

Conclusions

In this work, several gel polymer electrolytes based on the co-polymer matrix PMH and ionic liquid $[Bmim]BF_4$ have been prepared by the solution casting method. The purpose using ionic liquid as the plasticizer is to improve the safety of gel polymer electrolyte since IL is non-volatile and inflammable. The dependence of the electrolyte properties on the composition is systematically studied. With the same amount of plasticizer, PMH_{12} exhibits low T_g and thus high ionic conductivity compared to PMH_7, since PMH_{12} with longer EO chains has better mobility than PMH_7. The existence of the ionic liquid in large quantity stabilizes the PMH_n-IL electrolyte. The gel film PMH_{12}(40%)/IL(60%) presents good mechanical properties and also exhibits relatively high conductivity ($1.13\times10^{-3}S\cdot cm^{-1}$ at 30 □) . In addition, this GPE shows good compatibility with metallic lithium. Furthermore, a coin cell based on this GPE, with $LiFePO_4$ as cathode and metallic lithium as anode, shows discharge capacities as high as 145 $mAh\cdot g^{-1}$ and 158 $mAh\cdot g^{-1}$ when cycled at 30 □ and 50 □, respectively, under the current rate of 0.1 C. Moreover, no obvious capacity fade is observed after 30 cycles at both temperatures.

Acknowledgements

This work was supported by Key Project of Natural Science Foundation of Jiangsu Province of China (Grant no. BK2011030), Key Project of Educational Commission of Jiangsu Province of China (Grant no. 11KJA430006) and the Priority Academic Program Development of Jiangsu Higher Education Institutions.

References

[1] M. Armand and J.M. Tarascon, Nature, 2008, 451, 652.

[2] H.J. Ha, E.H. Kil, Y.H. Kwon, J.Y. Kim, C. K. Lee and S.Y. Lee, Energy & Environmental Science, 2012, 5, 6491.

[3] P. Judeinstein and F. Roussel, Advanced Materials, 2005, 17, 723.

[4] E. Quartarone and P. Mustarelli, Chem. Soc. Rev. 2011, 40, 2525.

[5] D. Saikia, Y.H. Chen, Y.C. Pan, J. Fang, L.D. Tsai, G.T.K. Fey and H.M. Kao, Journal of Materials Chemistry, 2011, 21, 10542.

[6] M. Higa, K. Yaguchi and R. Kitani, Electrochimica Acta, 2010, 55, 1380.

[7] W.H. Hou and C.Y. Chen, Electrochimica Acta, 2004, 49, 2105.

[8] W.H. Hou, C.Y. Chen and C.C. Wang, Polymer, 2003, 44, 2983.

[9] S.M. Lee, W.L. Yeh, C.C. Wang and C.Y. Chen, Electrochimica Acta, 2004,49, 2667.

[10] P. Gavelin, R. Ljungback, P. Jannasch and B. Wesslen, Solid State Ionics, 2002,147, 325.

[11] X. Zuo, X.M. Liu, F. Cai, H. Yang, X.D. Shen and G. Liu, Journal of Materials Chemistry, 2012, 22, 22265.

[12] X. Zuo, X.M. Liu, F. Cai, H. Yang, X.D. Shen and G. Liu, Journal of Power Sources, 2013, 239, 111.

[13] K.M. Abraham and Z. Jiang, Journal of Electrochemical Society, 1997,144, L136.

[14] F. Groce, F. Gerace, G. Dautzemberg, S. Passerini, G.B. Appetecche and B. Scrosai, Electrochimca Acta, 1994, 39, 2187.

[15] I. Kelly, J.F. Owen and B.C.H. Steele, Journal of Materials Chemistry, 1984 ,168, 467.

[16] Y. Ito, K. Kanehori, K. Miyauchi and T. Kudo, Journal of Materials Science, 1987, 22, 1845.

[17] K.M. Abraham, M. Alamgir and R.K. Reynolds, Journal of Electrochemical Society, 1988, 135, 535.

[18] L. Yang, J. Lin, Z. Wang, C. Wang, R. Zhou and Q. Liu, Solid State Ionics, 1990,40, 616.

[19] K.M. Abraham, Z. Jiang and B. Carroll, Chemistry of Materials, 1997, 9, 1978.

[20] Y.S. Ye, J. Rick and B. J. Hwang, Journal of Materials Chemistry A, 2013, 1, 2719.

[21] F. Cai, X. Zuo, X.M. Liu, L. Wang, W. Zhai and H. Yang, Electrochimca Acta, 2013, 106, 209.

[22] J. Evans, C. A. Vincent, P. G. Bruce, Polymer, 1987, 28, 2324.

[23] K. M. Abraham, Z. Jiang, B. Carroll, Chem. Mater., 1997, 9, 1978.

[24] S.A. Katsyuba, E.E. Zvereva, A.Vidis and P. J. Dyson, The Journal of Chemical Physics A, 2007, 111, 352.

[25] Y. Masuda, M. Seki, M. Nakayama, M. Wakihara and H. Mita, Solid State Ionics, 2006, 177, 843.

[26] T. Nishida , Y. Tashiro and M. Yamamoto, The Journal of Chemical Physics, 2003, 120, 135.

[27] T. Nishida, Y. Tashiro, M. Yamamoto, J. Fluorine Chem., 2003, 120, 135

[28] Shalu, S.K. Chaurasia, R.K. Singh and S. Chandra, The Journal of Chemical Physics B, 2013, 117, 897.

[29] H.H. Zheng, Chemical Industry Press Beijing ,2007, 169.

[30] Y.M Lee, D.H. Ko, J.Y Lee and J.K Park, Electrochimica Acta, 2006, 52, 1582.

[31] T. Niitani, M. Shimada, K. Kawamura and K. Kanamura, Journal of Power Sources, 2005, 146, 386.

[32] W. Xu, K.S. Siow, Z.Q. Gao and S.Y. Lee, Solid State Ionics, 1998, 112, 1.

[33] A.M. Stephan, Y. Saito, N. Muniyandi, N.G. Renganathan, S. Kalyanasundaram and R.N. Elizabeth, Solid State Ionics, 2002, 148, 467.

[34] Y. Kang, H.J. Kim, E. Kim, B. Oh and J.H. Cho, Journal of Power Sources, 2001, 92, 255.

[35] G. H. Lane, Electrochimica Acta, 2012, 83, 513.

[36] S.Y. Chew, J. Sun, J. Wang, H.K. Liu, M. Forsyth and D.R. MacFarlane, Electrochimica Acta, 2008, 53, 6460.

[37] Q. Hu, S. Osswald, R. Daniel, Y. Zhu, S. Wesel, L. Ortiz and D.R. Sadoway, Journal of Power Sources, 2011,196, 5604.

[38] K. Hayamizu, Y. Aihara, H. Nakagawa, T. Nukuda and W.S. Price, The Journal of Chemical Physics B, 2004, 108, 19527.

[39] H. Ye, J. Huang, J.J. Xu, A. Khalfan and S. G. Greenbaum, Journal of Electrochemical Society, 2007, 154, A1048.

[40] H.S. Jeong and S.Y. Lee, Journal of Power Sources, 2011, 196, 6716.

[41] N.S. Choi and J.K. Park, Electrochimica Acta, 2001, 46, 1453.

Table 1. The data related to Li^+ transference number of electrolytes at [Li]:[EO]=1:20.

Fig. 1 Chemical structures of macro-monomers, (a) MPEGM, (b) HPEGM.

Fig. 2 IR spectra of [Bmim]BF_4 (Bu: Butyl Me: Methyl).

Fig. 3 The structural formula of [Bmim]BF_4

Fig. 4 DSC traces for polymer electrolytes, (a) the different GPEs with the same concentration of Lithium salt, (b) the PMH_{12}-60 electrolyte with various concentration of lithium salt.

Fig. 5 (a) The TG profiles for IL, PMH_7, and several PMH_7 based gel polymer electrolytes; (b) The TG profiles for IL, PMH_{12}, and several PMH_{12} based gel polymer electrolytes.

Fig. 6 Temperature dependence of ionic conductivity of polymer electrolytes (a) PMH_7-IL and (b) PMH_{12}-IL

Fig. 7 Impedance spectra of the Li/PMH_{12}-60/Li cell measured before and after polarization at 30 □. Inserted figure: depolarization curve of the cell .

Fig. 8 (a) Impedance profiles of Li/PMH_{12}-60 /Li, (b) the change in the area specific bulk and interface resistances (R_{bulk} and R_{intf}) as a function of storage time.

Fig. 9 Electrochemical stability of the polymer electrolytes

Fig. 10 Cycle life test of Li/PMH_{12}-60/$LiFeO_4$ cell at 0.1 C. Inserted figure: Charge-discharge curves of Li/PMH_{12}-60/$LiFePO_4$ cell. (a) at 30 □, (b) 50 □.

Table 1. The data related to Li^+ transference number of electrolytes at [Li]:[EO]=1:20.

Electrolyte	$R_{b,0}(\Omega)$	$R_{b,s}(\Omega)$	$R_{i,0}(\Omega)$	$R_{i,s}(\Omega)$	I_0(mA)	I_s(mA)	t^+
PMH_7	226.4	241.9	673.8	890.4	0.046	0.022	0.26
PMH_{12}	233.7	238.5	683.2	873.4	0.051	0.026	0.28
PMH_7-30	168.5	205.2	604.8	779.4	0.025	0.006	0.23
PMH_7-60	182.7	229.4	653.6	802.5	0.029	0.009	0.30
PMH_7-70	178.3	223.2	628.9	822.4	0.031	0.011	0.32
PMH_{12}-30	150.2	198.7	562.0	725.3	0.028	0.008	0.29
PMH_{12}-60	170.4	212.2	609.3	798.3	0.024	0.008	0.33
PMH_{12}-70	225.8	296.1	743.7	926.3	0.035	0.014	0.35

Fig. 1

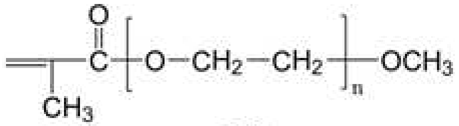

n=7, 12

a MPEGM

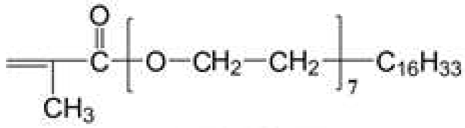

b HPEGM

Fig. 2

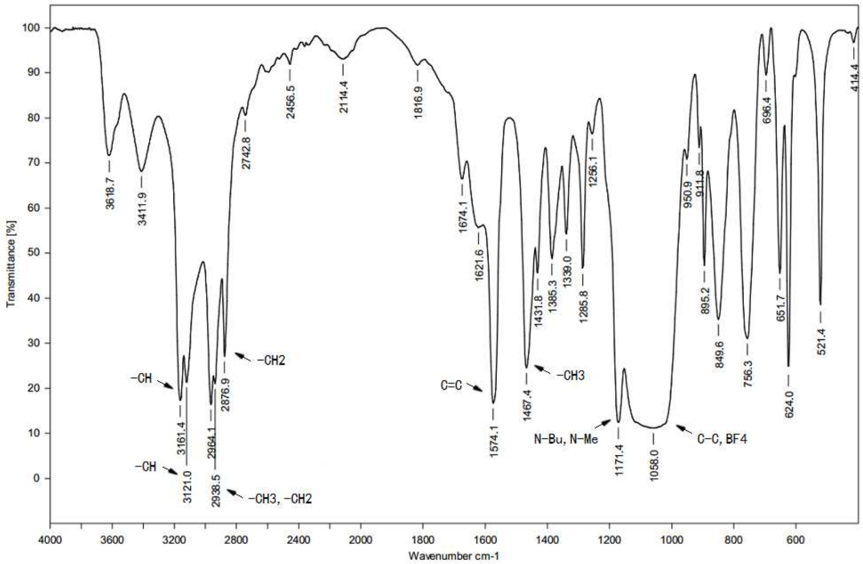
Transmittance [%]
Wavenumber cm-1
3618.7
3411.9
3161.4
3121.0
2964.1
2938.5
2876.9
2742.8
2456.5
2114.4
1816.9
1674.1
1621.6
1574.1
1467.4
1431.8
1385.3
1339.0
1285.8
1256.1
1171.4
1058.0
950.9
911.8
895.2
849.6
756.3
696.4
651.7
624.0
521.4
414.4
−CH
−CH
−CH2
−CH3, −CH2
C=C
−CH3
N−Bu, N−Me
C−C, BF4
100
90
80
70
60
50
40
30
20
10
0
4000
3600
3200
2800
2400
2000
1800
1600
1400
1200
1000
800
600

Fig. 3

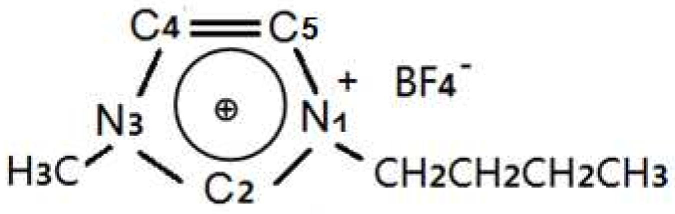

Fig.4 (a)

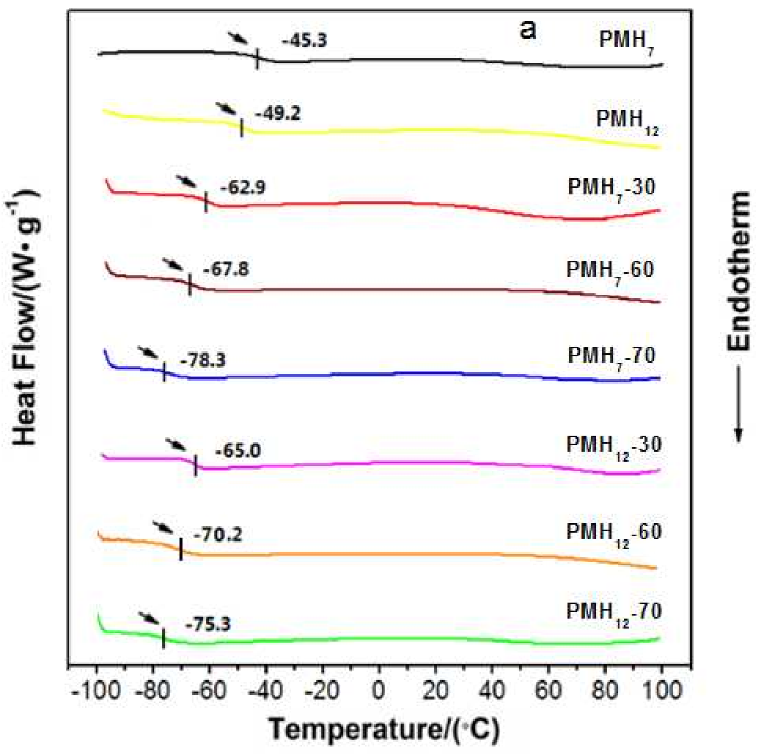
a
PMH$_7$
-45.3
PMH$_{12}$
-49.2
PMH$_7$-30
-62.9
PMH$_7$-60
-67.8
PMH$_7$-70
-78.3
PMH$_{12}$-30
-65.0
PMH$_{12}$-60
-70.2
PMH$_{12}$-70
-75.3
Heat Flow/(W·g^{-1})
Endotherm
-100 -80 -60 -40 -20 0 20 40 60 80 100
Temperature/(°C)

Fig.4 (b)

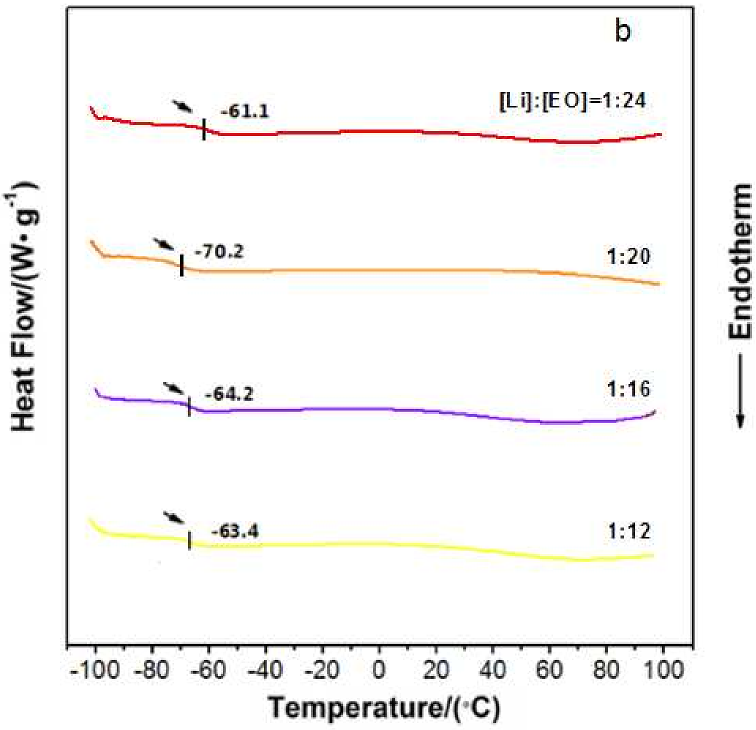
b
[Li]:[EO]=1:24
-61.1
1:20
-70.2
1:16
-64.2
1:12
-63.4
Heat Flow/(W•g^{-1})
Endotherm
-100
-80
-60
-40
-20
0
20
40
60
80
100
Temperature/(°C)

Fig. 5 (a)

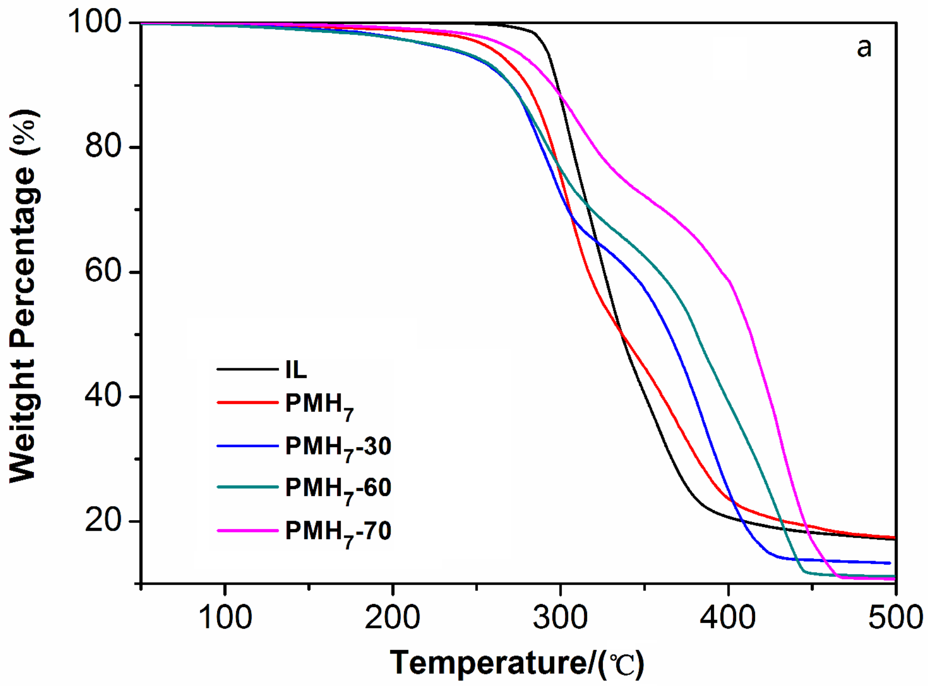
100
80
60
40
20
Weitght Percentage (%)
100
200
300
400
500
Temperature/(℃)
a
IL
PMH$_7$
PMH$_7$-30
PMH$_7$-60
PMH$_7$-70

Fig.5 (b)

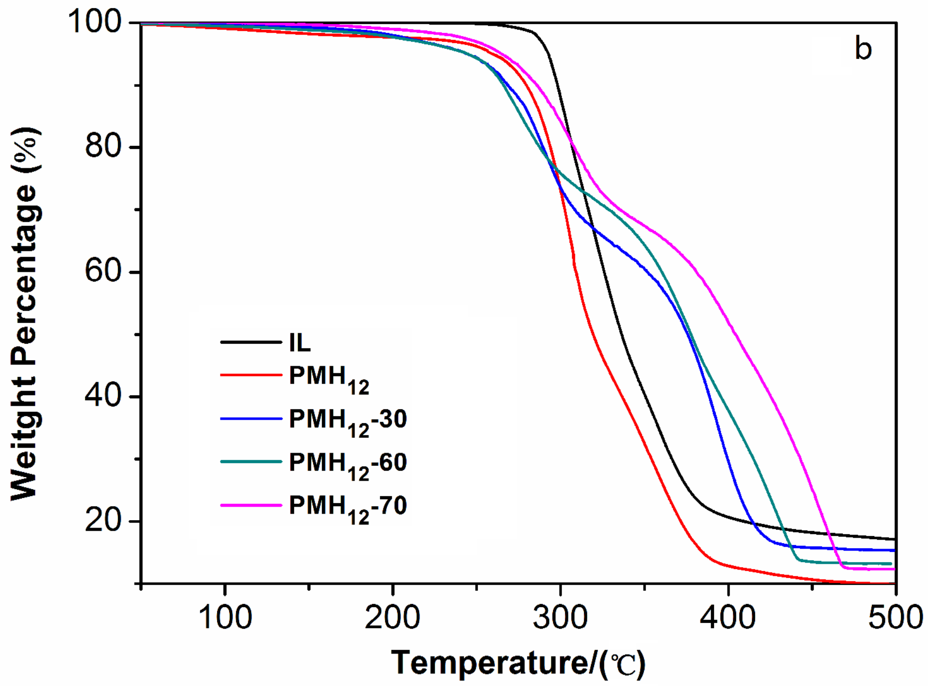
b
Weitght Percentage (%)
Temperature/(℃)
100
80
60
40
20
100
200
300
400
500
IL
PMH12
PMH12-30
PMH12-60
PMH12-70

Fig.6 (a)

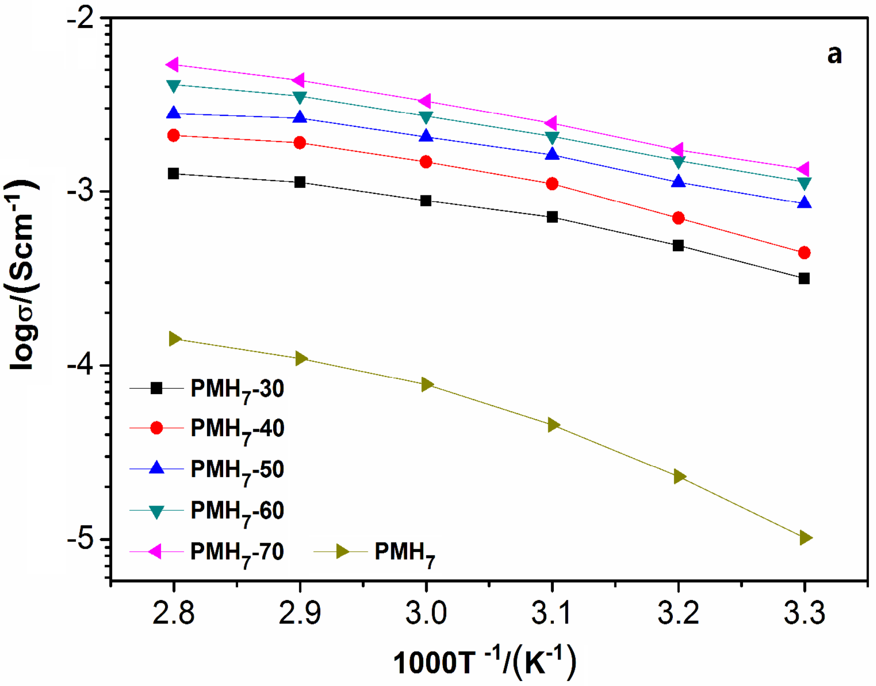
a
-2
-3
-4
-5
log σ/(Scm^{-1})
2.8
2.9
3.0
3.1
3.2
3.3
1000T^{-1}/(K^{-1})
PMH$_7$-30
PMH$_7$-40
PMH$_7$-50
PMH$_7$-60
PMH$_7$-70
PMH$_7$

Fig.6 (b)

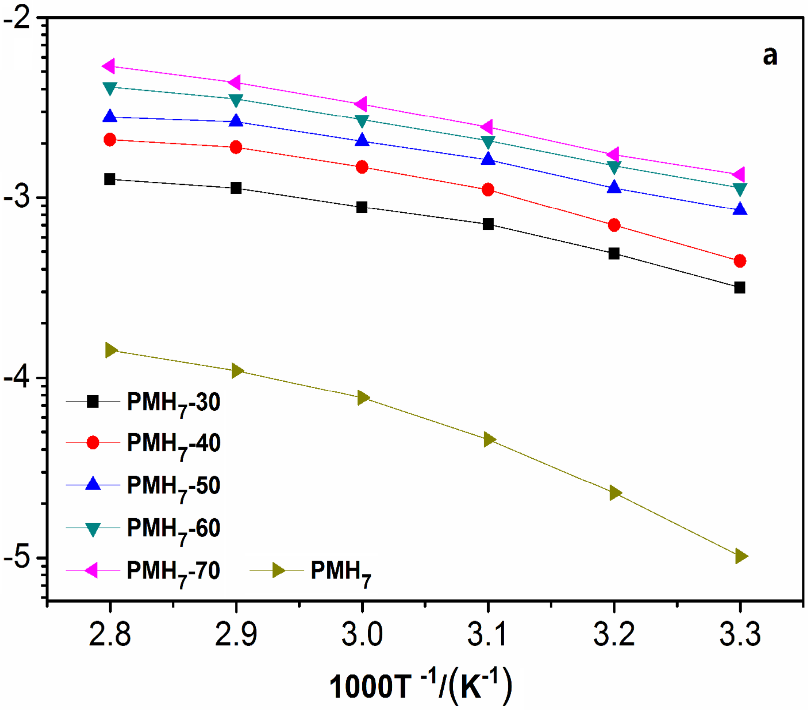
a
logσ/(Scm^{-1})
-2
-3
-4
-5
2.8
2.9
3.0
3.1
3.2
3.3
1000T $^{-1}$/(K^{-1})
PMH$_7$-30
PMH$_7$-40
PMH$_7$-50
PMH$_7$-60
PMH$_7$-70
PMH$_7$

Fig. 7

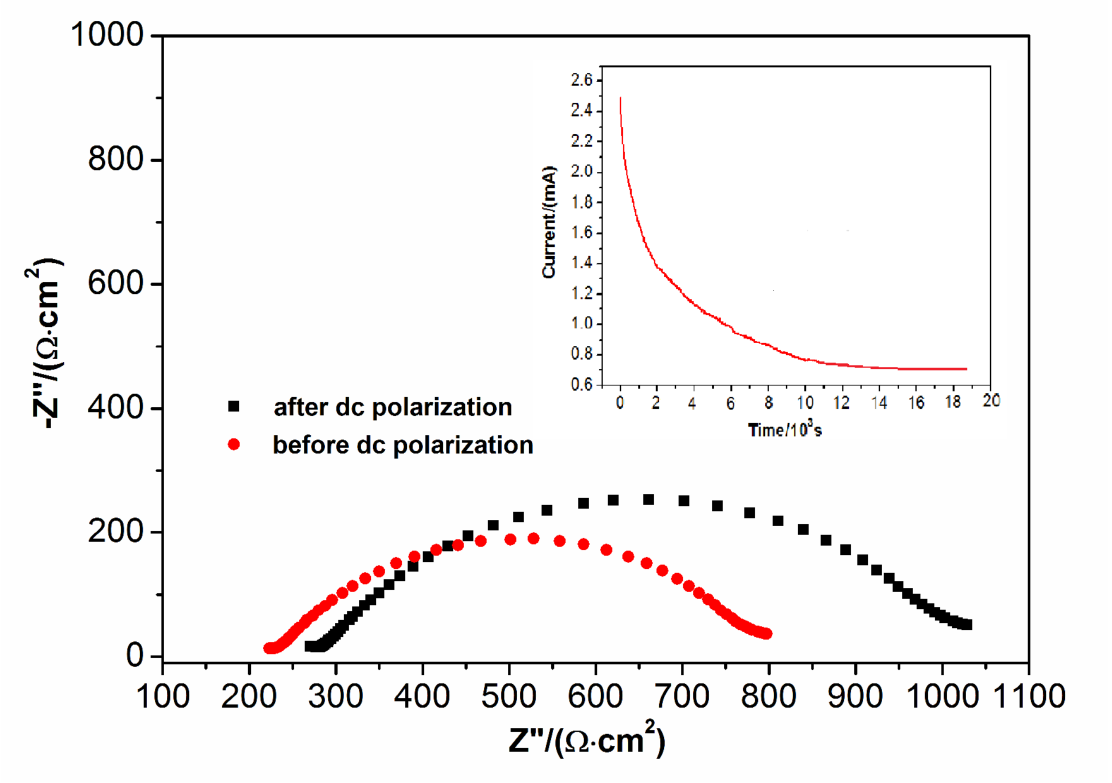
1000
800
600
400
200
0
-Z''/(Ω·cm^2)
100 200 300 400 500 600 700 800 900 1000 1100
Z''/(Ω·cm^2)
■ after dc polarization
● before dc polarization
Current /(mA)
2.6
2.4
2.2
2.0
1.8
1.6
1.4
1.2
1.0
0.8
0.6
0 2 4 6 8 10 12 14 16 18 20
Time/10^{3}s

Fig. 8 (a)

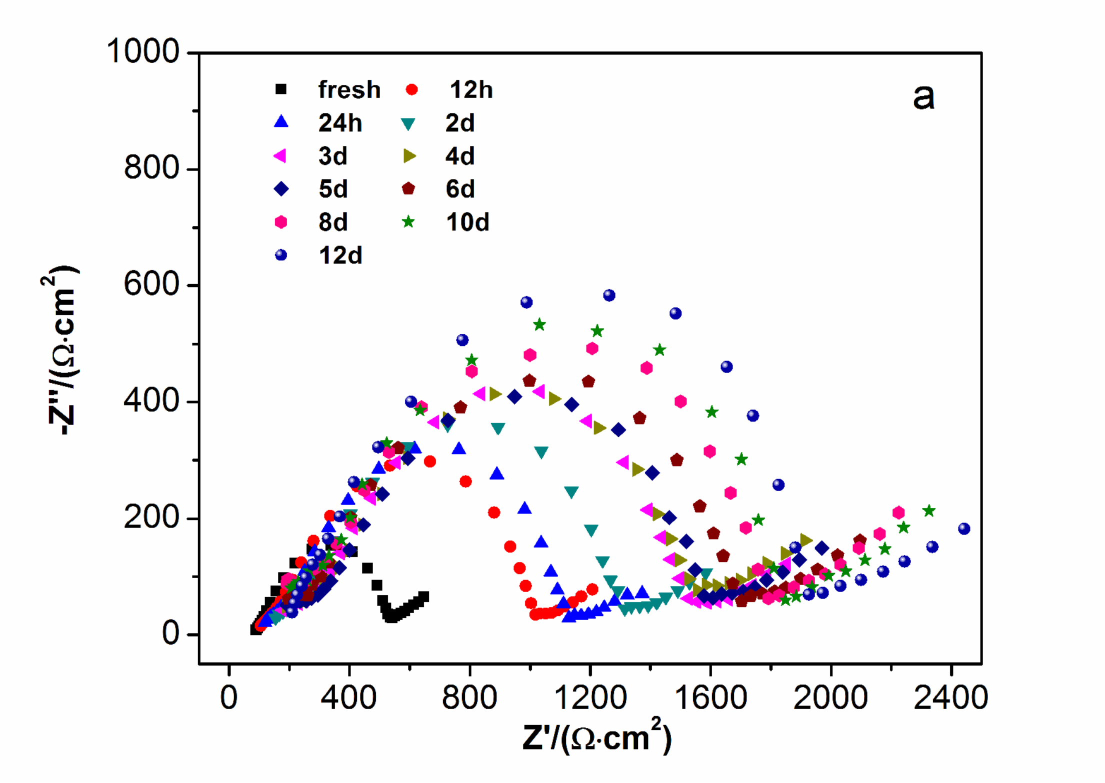
a
fresh
12h
24h
2d
3d
4d
5d
6d
8d
10d
12d
-Z''/(Ω·cm²)
Z'/(Ω·cm²)
0
200
400
600
800
1000
0
400
800
1200
1600
2000
2400

Fig. 8 (b)

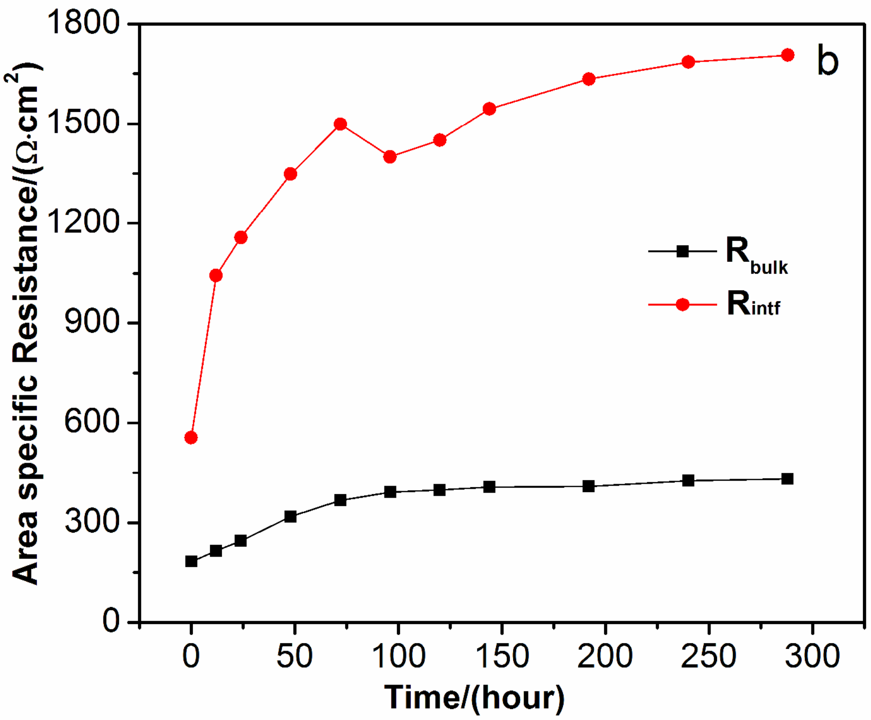
b
Area specific Resistance/(Ω·cm^2)
0
300
600
900
1200
1500
1800
Time/(hour)
0
50
100
150
200
250
300
R$_{bulk}$
R$_{intf}$

Fig. 9

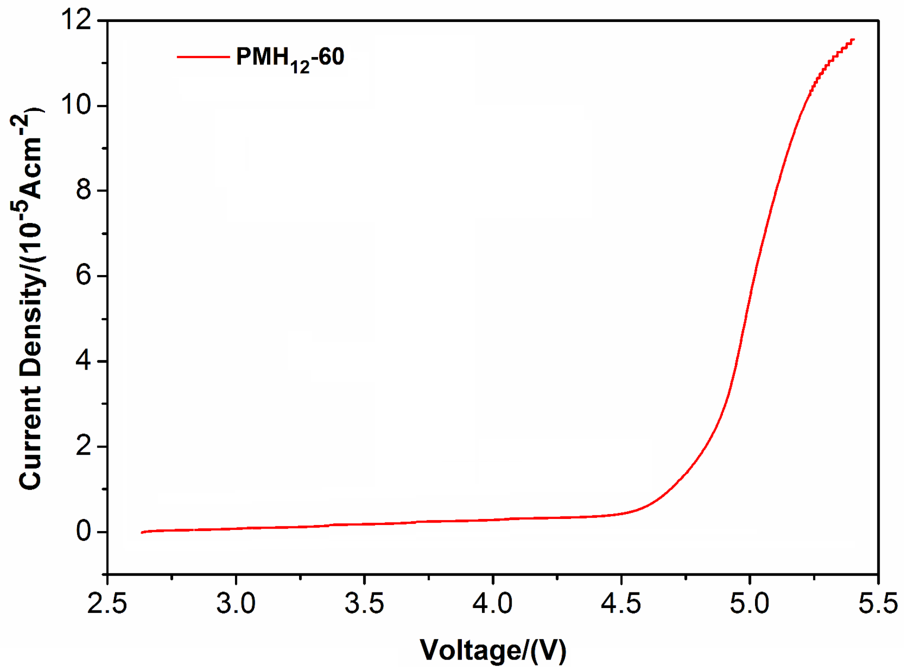
PMH12-60
Current Density/(10-5Acm-2)
Voltage/(V)
0
2
4
6
8
10
12
2.5
3.0
3.5
4.0
4.5
5.0
5.5

Fig. 10 (a)

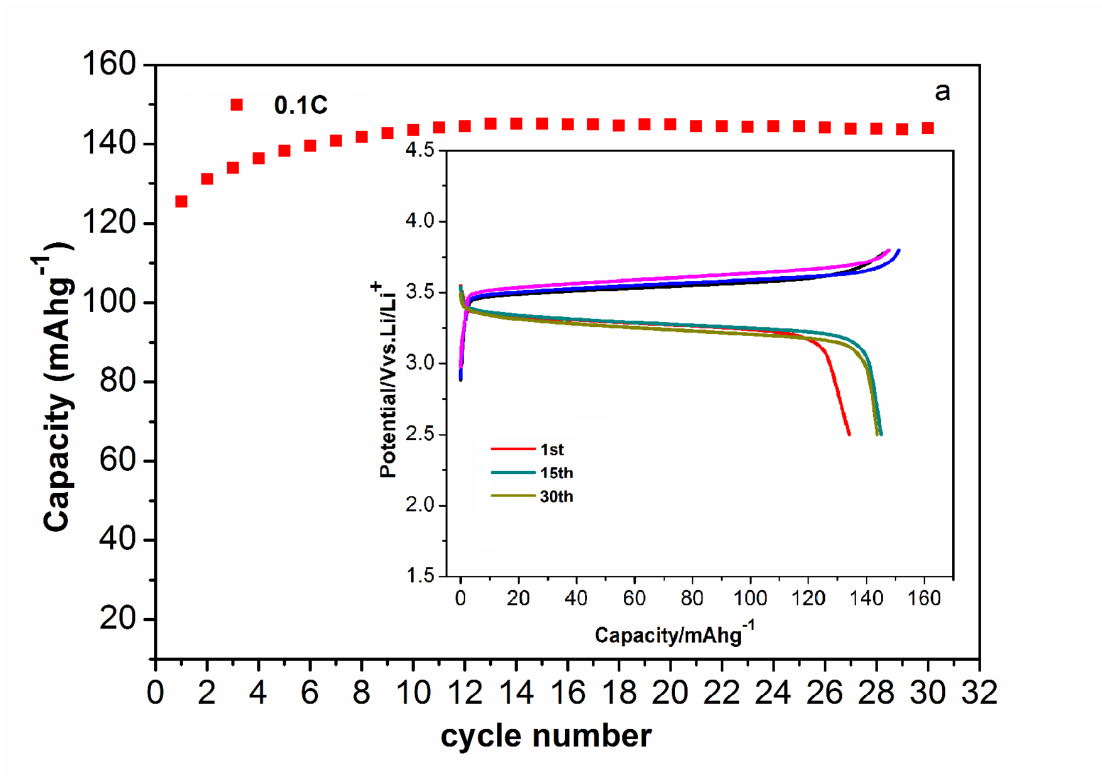

a
0.1C
Capacity (mAhg^{-1})
cycle number
160
140
120
100
80
60
40
20
0 2 4 6 8 10 12 14 16 18 20 22 24 26 28 30 32
Potential/Vvs.Li/Li^{+}
Capacity/mAhg^{-1}
4.5
4.0
3.5
3.0
2.5
2.0
1.5
0 20 40 60 80 100 120 140 160
1st
15th
30th

Fig.10 (b)

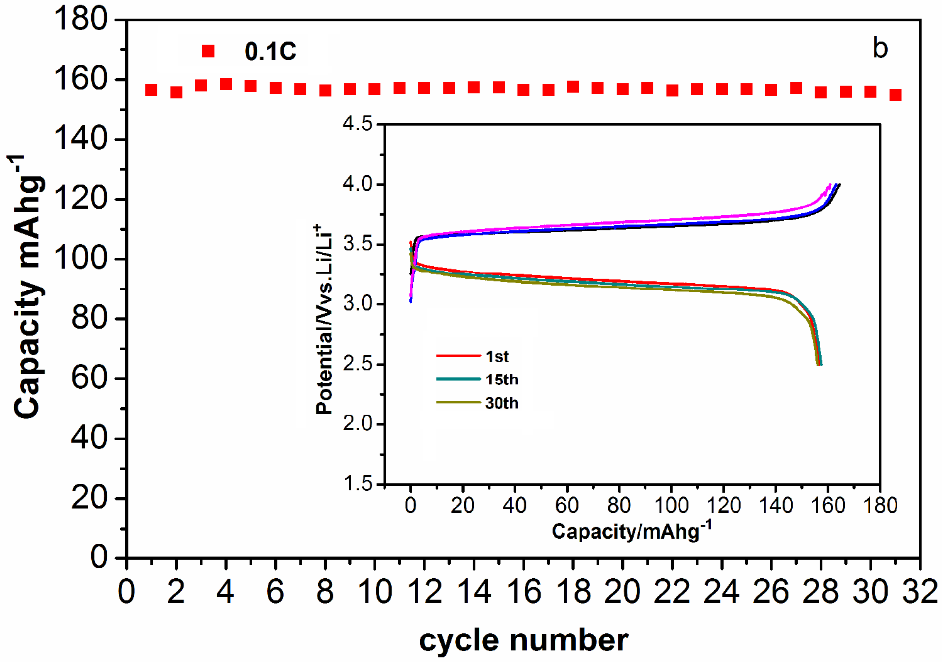
0.1C
b
Capacity mAhg^{-1}
0
20
40
60
80
100
120
140
160
180
cycle number
0 2 4 6 8 10 12 14 16 18 20 22 24 26 28 30 32
Potential/Vvs.Li/Li$^+$
1.5
2.0
2.5
3.0
3.5
4.0
4.5
1st
15th
30th
Capacity/mAhg^{-1}
0 20 40 60 80 100 120 140 160 180